 DOI: 10.17344/acsi.2016.2589

Scientific paper

4-Fluoro-*N*'-(2-hydroxy-3-methoxybenzylidene) benzohydrazide and its Oxidovanadium(V) Complex: Syntheses, Crystal Structures and Insulin-enhancing Activity

Jin-Xian Lei,[1,*] Jing Wang,[1,2] Yang Huo[2] and Zhonglu You[2,*]

[1] *College of Chemistry and Chemical Engineering, Jinzhong University, Jinzhong 030619, P. R. China*

[2] *College of Chemistry and Chemical Engineering, Liaoning Normal University, Dalian 116029, P. R. China*

** Corresponding author: E-mail: leijinxianjz@sohu.com; youzhonglu@126.com*

Received: 15-05-2016

Abstract

A hydrated hydrazone compound, 4-fluoro-*N*'-(2-hydroxy-3-methoxybenzylidene)benzohydrazide monohydrate ($H_2L \cdot H_2O$), was prepared and characterized by elemental analysis, HRMS, IR, UV-Vis and ^{1}H NMR spectroscopy. Reaction of H_2L, kojic acid (5-hydroxy-2-(hydroxymethyl)-4*H*-pyran-4-one; Hka) and $VO(acac)_2$ in methanol afforded a novel oxidovanadium(V) complex, [VO(ka)L]. The complex was characterized by elemental analysis, IR, UV-Vis and ^{1}H NMR spectroscopy. Thermal analysis was also performed. Structures of H_2L and the complex were further confirmed by single crystal structural X-ray diffraction. The vanadium complex is the first structurally characterized vanadium complex of kojic acid. Insulin-mimetic tests on C2C12 muscle cells indicate that the complex significantly stimulated cell glucose utilization with cytotoxicity at 0.11 g L^{-1}.

Keywords: Oxidovanadium complex, Kojic acid, Hydrazone, Crystal structure, Insulin-enhancing activity

1. Introduction

Since 1980s, inorganic vanadium salts and vanadium complexes with various ligands have been reported to possess potent pharmacological effects of insulin-mimetic activity.[1–4] Studies indicated that vanadium compounds improve not only hyperglycemia in human subjects and animal models of type I diabetes but also glucose homeostasis in type II diabetes.[5,6] However, the inorganic vanadium salts are considered as less active and more toxic. In order to reduce the side effects of inorganic vanadium salts, vanadium complexes with various organic ligands have received particular attention and demonstrated to be effective.[7–9] Among the complexes, bis(maltolato)oxovanadium(IV) (BMOV),[10] synthesized by simple metathesis of vanadyl sulfate trihydrate and maltol (3-hydroxy-2-methyl-4-pyrone), has important and interesting insulin-enhancing activity.[11,12] Yet, there are some side effects of BMOV, principally diarrhea.[13] Schiff bases play important role in biological chemistry. Several vanadium complexes derived from Schiff bases have shown to normalize blood glucose level with high efficiency and low toxicity, even at low concentration.[14,15] Schiff bases with hydrazone type are of particular interest due to their biological properties.[16–20] In recent years, a number of vanadium complexes were prepared from tridentate hydrazones, because of their excellent coordination ability and facilitate preparation. In view of the increasing importance of vanadium complexes with hydrazone type Schiff bases, we report herein the synthesis, characterization, and insulin-enhancing activity of a novel oxidovanadium(V) complex with the hydrazone compound 4-fluoro-*N*'-(2-hy-

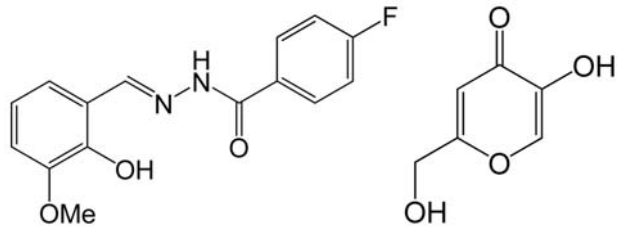

Scheme 1. H_2L and Hka

droxy-3-methoxybenzylidene)benzohydrazide monohydrate ($H_2L \cdot H_2O$; Scheme 1) and maltol analogous compound kojic acid (5-hydroxy-2-(hydroxymethyl)-4*H*-pyran-4-one; Hka; Scheme 1). The vanadium complex is the first structurally characterized vanadium complex of kojic acid.

2. Experimental

2. 1. Materials and Measurements

Starting material, reagents and solvents were purchased from commercial suppliers and used as received. Elemental analyses were performed on a Perkin-Elmer 240C elemental analyzer. IR spectra were recorded on a Jasco FT/IR-4000 spectrometer as KBr pellets in the 4000–400 cm^{-1} region. Electronic spectra were recorded on a Lambda 10 spectrometer. Absorbance was recorded on a Bio-Tek model ELx800 96-well plate reader. HRMS data was obtained with ESI (electrospray ionization) mode. ^{1}H NMR data were recorded on Bruker 300 MHz spectrometer. X-ray diffraction was carried out on a Bruker SMART 1000 CCD diffractometer.

2. 2. Preparation of $H_2L \cdot H_2O$

To a methanolic solution (20 mL) of 3-methoxysalicylaldehyde (0.152 g, 1.00 mmol) was added a methanolic solution (20 mL) of 4-fluorobenzohydrazide (0.154 g, 1.00 mmol) with stirring. The mixture was stirred for 10 min at room temperature and filtered. Upon keeping the filtrate in air for a few days, colorless block-shaped crystals of the compound, suitable for X-ray crystal structure determination, were formed at the bottom of the vessel on slow evaporation of the solvent. The crystals were isolated, washed with MeOH and dried in a vacuum desiccator containing anhydrous $CaCl_2$. Yield: 91%. Analysis: Calcd. for $C_{15}H_{15}FN_2O_4$: C, 58.82; H, 4.94; N, 9.15%. Found: C, 58.69; H, 5.03; N, 9.06%. IR data (KBr, cm^{-1}): 3550 m, 3418 w, 3210 w, 1652 s, 1609 s, 1507 w, 1470 m, 1368 w, 1325 w, 1282 m, 1241 s, 1162 w, 1103 w, 1069 w, 965 w, 893 w, 853 m, 764 w, 730 m, 668 w, 637 w, 610 w, 502 w. UV-Vis [methanol, λ/nm ($å$/L·mol^{-1}·cm^{-1})]: 298 (21,220), 338 (5,130). HRMS (ESI): m/z calcd for $C_{15}H_{14}FN_2O_3$ $[M + 1]^+$ 289.0983; found: 289.0986. ^{1}H NMR (300 MHz, d^6-DMSO): δ 12.11 (s, 1H, N*H*), 10.93 (s, 1H, O*H*), 8.67 (s, 1H, C*H*=N), 8.03 (d, 2H, Ar*H*), 7.41 (d, 2H, Ar*H*), 7.18 (d, 1H, Ar*H*), 7.06 (d, 1H, Ar*H*), 6.89 (t, 1H, Ar*H*), 3.84 (s, 3H, CH_3).

2. 3. Preparation of the Complex

A methanolic solution (30 mL) of $VO(acac)_2$ (0.27 g, 1.0 mmol) was added to a methanolic solution (20 mL) of H_2L (0.288 g, 1.00 mmol) and kojic acid (0.142 g, 1.00 mmol) with stirring. The mixture was stirred at room temperature for 30 min to give deep brown solution. The resulting solution was allowed to stand in air for a few days until three quarters of the solvent was evaporated. Brown block-shaped single crystals of the complex suitable for X-ray single crystal diffraction were formed at the bottom of the vessel. The crystals were isolated by filtration, washed three times with cold methanol and dried in a vacuum desiccator containing anhydrous $CaCl_2$. Yield: 62%. Analysis: Calcd. for $C_{21}H_{16}FN_2O_8V$: C, 51.03; H, 3.26; N, 5.67%. Found: C, 50.86; H, 3.35; N, 5.76%. IR data (KBr, cm^{-1}): 3481 m, 1600 s, 1560 m, 1504 m, 1449 m, 1341 m, 1264 s, 1223 s, 1153 w, 1097 w, 1036 w, 972 s, 915 w, 863 m, 736 m, 650 w, 595 w, 558 w, 511 w, 434 w. UV-Vis [acetonitrile, λ/nm ($å$/L·mol^{-1}·cm^{-1})]: 215 (23,530), 280 (19,220), 354 (7,285), 460 (4,175). ^{1}H NMR (300 MHz, d^6-DMSO): δ 9.22 (s, 1H, Ar*H*), 8.65 (s, 1H, C*H*=N), 7.92 (d, 2H, Ar*H*), 7.45 (d, 2H, Ar*H*), 7.30 (d, 1H, Ar*H*), 7.06 (d, 1H, Ar*H*), 6.65 (m, 1H, Ar*H*), 5.84 (s, 1H, Ar*H*), 4.46 (s, 2H, CH_2), 3.81 (s, 3H, CH_3).

2. 4. X-ray Crystallography

Diffraction intensities for $H_2L{\cdot}H_2O$ and the complex were collected at 298(2) K using a Bruker SMART 1000 CCD area-detector diffractometer with Mo Kα radiation (λ = 0.71073 Å) for $H_2L{\cdot}H_2O$ and Cu Kα radiation (λ = 1.54178 Å) for the complex. The crystals were mounted on the top of thin glass fibers. The collected data were re-

Table 1 Crystallographical and experimental data for $H_2L{\cdot}H_2O$ and the complex

	$H_2L \cdot H_2O$	The complex
Formula	$C_{15}H_{15}FN_2O_4$	$C_{21}H_{16}FN_2O_8V$
Mr	306.29	494.30
Crystal size/mm^3	0.20 × 0.18 × 0.13	0.33 × 0.30 × 0.28
Crystal system	Orthorhombic	Orthorhombic
Space group	$P2_12_12_1$	*Pbca*
a /Å	4.7985(4)	8.6357(3)
b /Å	13.0361(11)	14.3372(5)
c /Å	22.8054(17)	32.6037(12)
V /Å^3	1426.6(2)	4036.7(2)
Z	4	8
D_c /(g cm^{-3})	1.426	1.627
μ /mm^{-1}	0.113	4.692
F(000)	640	2016
Measured reflections	2533	4008
Observed reflections [$I \geq 2\sigma(I)$]	2165	3262
Data/restraints/ parameters	2533/4/210	4008/0/300
Goodness-of-fit on F^2	1.055	1.080
R_1, wR_2 [$I \geq 2\sigma(I)$][a]	0.0323, 0.0697	0.0485, 0.1199
R_1, wR_2 (all data)[a]	0.0441, 0.0742	0.0615, 0.1271
Large diff. peak and hole /(e Å^{-3})	0.114 and –0.127	0.809 and –0.421

[a] $R_1 = \Sigma||Fo|-|Fc||/\Sigma|Fo|$, $wR_2 = [\Sigma w(Fo^2 - Fc^2)^2/\Sigma w(Fo^2)^2]^{1/2}$.

duced with SAINT,[21] and multi-scan absorption correction was performed using SADABS.[22] Structures of $H_2L \cdot H_2O$ and the complex were solved by direct methods, and refined against F^2 by full-matrix least-squares methods using SHELXTL.[23] All non-hydrogen atoms were refined anisotropically. The amino and water hydrogen atoms in $H_2L \cdot H_2O$ were located from a difference Fourier map and refined isotropically, with N–H and O–H distances restrained to 0.86(2) and 0.82(2) Å, respectively. The remaining hydrogen atoms were placed in calculated positions and constrained to ride on their parent atoms. Crystallographic data for $H_2L \cdot H_2O$ and the complex are summarized in Table 1.

2. 5. Cell Culture and Viable Cell Counts

The biological assay was determined according to the literature method.[14] In general, C2C12 mouse skeletal muscle cells were cultured in Dulbecco modified Eagle's medium with 4 mmol L^{-1} *L*-glutamine adjusted to contain 1.5 g L^{-1} Na_2CO_3, 4.5 g L^{-1} glucose, and 10% fetal bovine serum in a humidified atmosphere of 5% CO_2 and 95% air at 37 °C. C2C12 cells were sub-cultured in log phase to 70% confluence and seeded at a density of 5000 cells per well into 96-well culture plates. To limit batch-to-batch variation, cell subcultures were limited to 10 passages. After three days culture myotube formation was induced by replacing the fetal bovine serum in the medium with 10% horse serum. All experiments were done in five days when more than 75% of the cells were differentiated morphologically. The cells were suspended in a trypan blue (0.1% w/w) phosphate buffered saline solution and the ratio of stained to non-stained cells was determined after 5 min of incubation time. Viable cell counts were performed using a hemocytometer.

2. 6. Glucose Uptake Determination

Three hours prior to glucose uptake, cells were incubated in glucose and serum-free media. On the 5th day, the medium was removed and replaced with 50 mL Dulbecco modified Eagle's medium without phenol red, which was supplemented with 8.0 mmol L^{-1} glucose and 0.1% bovine serum albumin containing either the complex at concentration of 0.10 g L^{-1} or the positive control, insulin, or metformin at 1.0 mmol L^{-1}. The plate was then incubated for 2 h at 37 °C and 5% CO_2. After incubation, 4.0 mL media was removed from each well and transferred to a new 96-well plate to which 196 mL deionized water was added in each well. A total of 50 mL of this diluted medium was transferred to a new 96-well plate and 50 mL of the prepared glucose assay reagent was added per well and incubated for 30 min at 37 °C. Absorbance was taken at 570 nm on a 96-well plate reader. The glucose concentration per well was calculated from a standard curve. Glucose utilization was determined by subtracting the glucose concentration left in the medium of the relevant wells following incubation to media not exposed to cells during incubation. All assays were performed in triplicate to minimize the error.

2. 7. Cytotoxicity Assay

MTT (3-(4,5-Dimethylthiazo)-2-yl)-2,5-diphenyltetrazolium bromide) was dissolved in phosphate-buffered saline without phenol red at a concentration of 2.0 g L^{-1}. Dulbecco modified Eagle's medium in the 96-well plate was refreshed with 200 mL of fresh media followed by addition of 50 mL of MTT solution to each well. The plate was wrapped in aluminium foil to prevent light and incubated at 37 °C for 4 h, after which the media with MTT was removed and replaced with 200 mL DMSO and 25 mL Sorensen's glycine buffer. Absorbance was read at 570 nm in a plate reader.

3. Results and Discussion

3. 1. General

The hydrazone compound $H_2L \cdot H_2O$ was readily prepared by the condensation reaction of 3-methoxysalicylaldehyde with 4-fluorobenzohydrazide in methanol. Facile reaction of $VO(acac)_2$ with H_2L and kojic acid in methanol afforded the oxidovanadium(V) complex. Crystals of $H_2L \cdot H_2O$ and the complex are stable in air at room temperature. Elemental analyses are in good agreement with the chemical formulae proposed for the compounds.

3. 2. Structure Description of $H_2L \cdot H_2O$

Fig. 1 gives perspective view of $H_2L{\cdot}H_2O$ together with the atomic labeling system. The compound contains a hydrazone molecule and a water molecule. The hydrazone molecule adopts *E* configuration with respect to the methylidene unit, which is isostructural with the chloro-substituted compound, 4-chloro-*N*'-(2-hydroxy-3-methoxybenzylidene)benzohydrazide.[24] The length of the C(7)–N(1) methylidene bond (1.286(2) Å) confirms it as a typical double bond (Table 2). The shorter length of the C(8)–N(2) bond (1.345(2) Å) and the longer length of the C(8)–O(2) bond (1.227(2) Å) for the –C(O)–NH– unit than usual, suggest the presence of conjugation effect in the molecule. The bond lengths in the compound are within normal values.[20,25,26] The dihedral angle between the two benzene rings is 14.8(3)°. In the crystal structure of the compound, hydrazone molecules are linked by water molecules through intermolecular O–H···O and N–H···O hydrogen bonds, to form two-dimensional sheets along *ab* plane (Table 3, Fig. 2). There is no obvious π···π interactions along *a* axis.

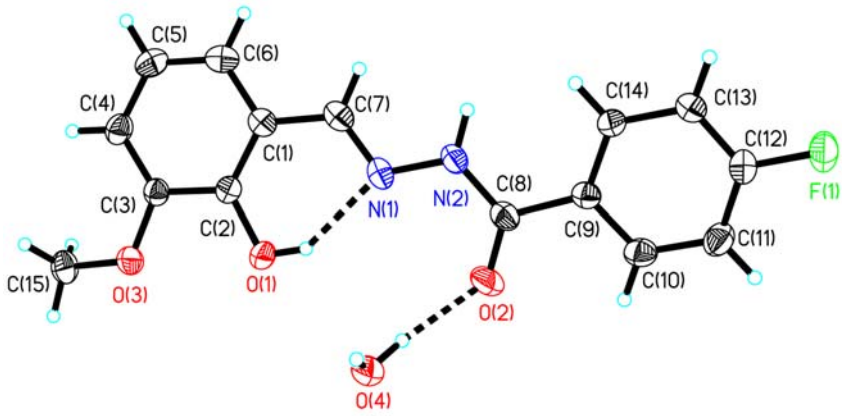

Figure 1. Molecular structure of $H_2L \cdot H2O$. Displacement ellipsoids are drawn at the 30% probability level and H atoms are shown as small spheres of arbitrary radii.

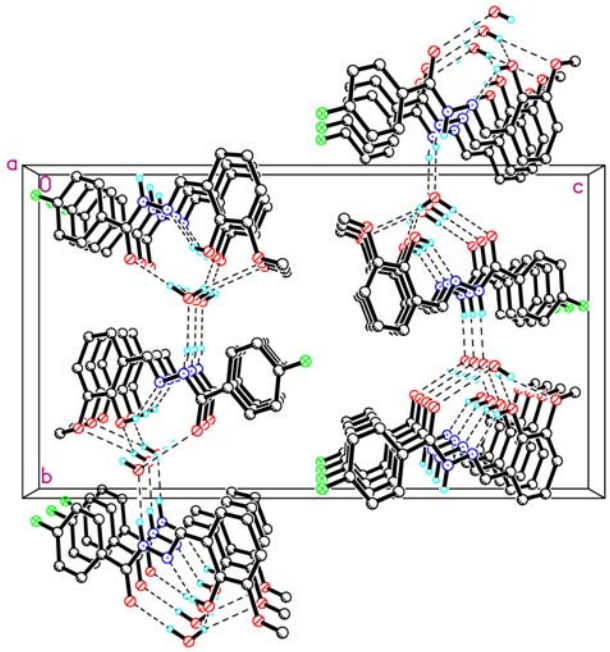

Figure 2. The crystal packing of $H_2L \cdot H_2O$, viewed along the *a* axis. Hydrogen bonds are shown as dashed lines.

3. 3. Structure Description of the Complex

Fig. 3 gives perspective view of the complex together with the atomic labeling system. The V atom in the complex is in an octahedral coordination, with the phenolate O, imino N, and enolate O atoms of the hydrazone ligand, and the deprotonated hydroxyl O atom of the kojic acid ligand defining the equatorial plane, and with one oxido O and the carbonyl O atom of the deprotonated kojic acid ligand locating at the axial positions. The V atom deviates from the least-squares plane defined by the equatorial atoms by 0.290(1) Å. The coordinative bond lengths in the complex are similar to those observed in vanadium complexes with hydrazone ligands.[27–31] Distortion of the octahedral coordination can be observed from the coordinative bond angles (Table 2), ranging from 74.84(8) to 103.54(8)° for the perpendicular angles, and from 153.05(9) to 174.94(10)° for the diagonal angles. The dihedral angle between the two benzene rings of the hydrazone ligand is 13.1(3)°. Upon coordination, the C(7)–N(1), N(1)–N(2) and C(8)–O(2) bonds of the complex are longer than those of the free hydrazone, while the N(2)–C(8) bond of the complex is shorter than that of the free hydrazone. This is caused by the tautomerization of the carbonyl form of the hydrazone ligand to the enolate form. In the crystal structure of the complex, adjacent complex molecules are linked through intermolecular O–H···O hydrogen bonds to form an infinite chain propagating along a axis (Table 3, Fig. 4). There are short π···π interactions along a axis (Table 4).

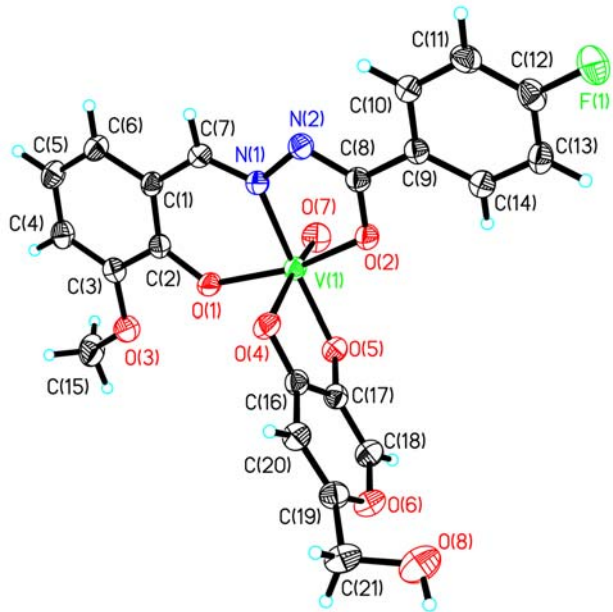

Figure 3. Molecular structure of the complex. Displacement ellipsoids are drawn at the 30% probability level and H atoms are shown as small spheres of arbitrary radii.

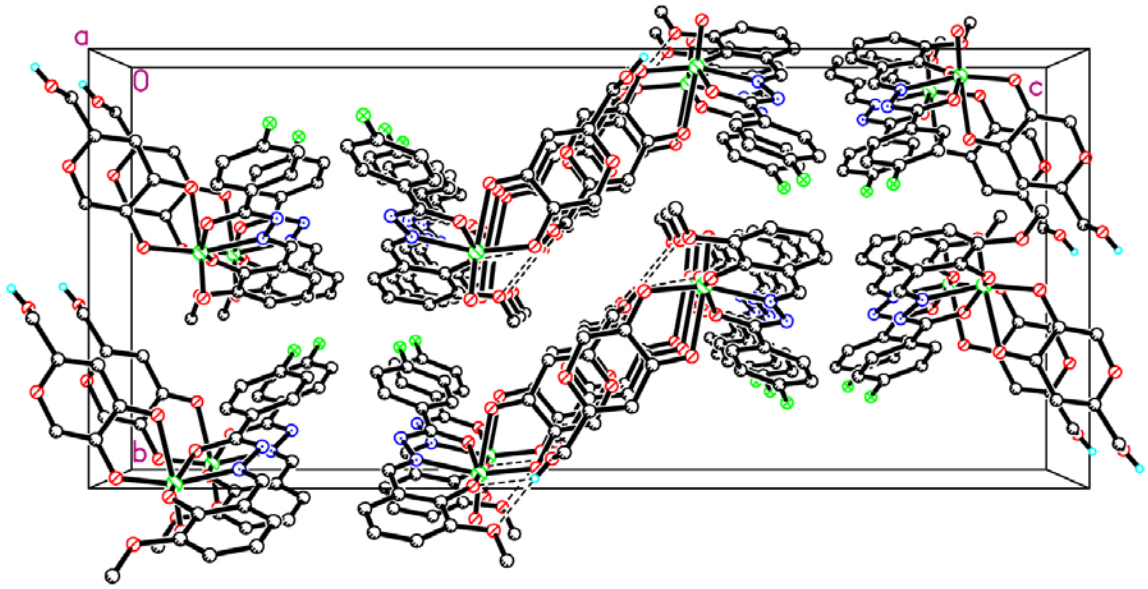

Figure 4. The crystal packing of the complex, viewed along the a axis. Hydrogen bonds are shown as dashed lines.

Table 2. Selected bond lengths (Å) and angles (°) for $H_2L \cdot H_2O$ and the complex

$H_2L \cdot H_2O$			
C(7)–N(1)	1.285(2)	N(1)–N(2)	1.3797(19)
N(2)–C(8)	1.345(2)	C(8)–O(2)	1.227(2)
The complex			
C(7)–N(1)	1.295(3)	N(1)–N(2)	1.394(3)
N(2)–C(8)	1.294(3)	C(8)–O(2)	1.314(3)
C(16)–O(4)	1.250(3)	C(17)–O(5)	1.350(3)
V(1)–O(1)	1.845(2)	V(1)–O(2)	1.941(2)
V(1)–O(5)	1.870(2)	V(1)–O(7)	1.580(2)
V(1)–O(4)	2.282(2)	V(1)–N(1)	2.084(2)
O(7)–V(1)–O(1)	99.52(11)	O(7)–V(1)–O(5)	97.49(10)
O(1)–V(1)–O(5)	103.54(8)	O(7)–V(1)–O(2)	99.72(11)
O(1)–V(1)–O(2)	153.05(9)	O(5)–V(1)–O(2)	92.45(8)
O(7)–V(1)–N(1)	98.18(11)	O(1)–V(1)–N(1)	83.89(8)
O(5)–V(1)–N(1)	161.27(9)	O(2)–V(1)–N(1)	74.84(8)
O(7)–V(1)–O(4)	174.94(10)	O(1)–V(1)–O(4)	81.97(9)
O(5)–V(1)–O(4)	77.44(7)	O(2)–V(1)–O(4)	80.51(8)
N(1)–V(1)–O(4)	86.77(8)		

Table 3. Hydrogen bond lengths (Å) and bond angles (°) for $H_2L \cdot H_2O$ and the complex

D*–H···*A	***d*(*D*–H)**	***d*(H···*A*)**	***d*(*D*···*A*)**	**Angle (*D*–H···*A*)**
$H_2L \cdot H_2O$				
O(1)–H(1)···N(1)	0.82	1.96	2.672(2)	145
O(4)–H(4A)vO(2)	0.83(1)	1.89(1)	2.708(2)	169(2)
N(2)–H(2)···O(4)^{i}	0.87(1)	2.02(1)	2.882(2)	170(2)
O(4)–H(4B)···O(1)^{ii}	0.82(1)	2.27(1)	3.002(2)	149(2)
O(4)–H(4B)···O(3)^{ii}	0.82(1)	2.47(2)	3.148(2)	142(2)
The complex				
O(8)–H(8)···O(1)^{iii}	0.82	2.44	3.025(4)	130(2)
O(8)–H(8)···O(3)^{iii}	0.82	2.15	2.923(4)	157(2)

Symmetry codes: (i) 1 – *x*, –1/2 + *y*, 1/2 – *z*; (ii) 1 + *x*, *y*, *z*; (iii) –1/2 + *x*, 3/2 – *y*, 1 – *z*.

Table 4 Parameters between the planes for the complex

Cg	*Cg*···*Cg* distance (Å)	Dihedral angle (°)	Perpendicular distance of *Cg*(I) on *Cg*(J) (Å)	Perpendicular distance of *Cg*(J) on *Cg*(I) (Å)	β(°)	γ(°)
Cg(1)-*Cg*(2)	4.787(3)	77.26	1.559	2.979	51.52	71.00
Cg(1)-*Cg*(3)^{iv}	4.684(3)	9.72	3.589	3.543	40.85	39.98
Cg(2)-*Cg*(2)^{v}	4.549(3)	44.14	3.898	4.105	25.54	31.03
Cg(3)-*Cg*(4)^{vi}	3.805(3)	13.24	3.475	3.657	16.05	24.04
Cg(4)-*Cg*(3)^{vii}	4.871(3)	52.73	1.567	4.479	23.13	71.23

Symmetry codes: (iv) 1 + *x*, *y*, *z*; (v) –1/2 + *x*, 1/2 – *y*, – *z*; (vi) –1 + *x*, *y*, *z*; (vii) 3/2 – *x*, –1/2 + *y*, *z*.

3. 4. IR and UV–Vis Spectra

The medium and broad absorption centered at 3550 and 3418 cm^{-1} in the spectrum of $H_2L \cdot H_2O$ and 3481 cm^{-1} in the spectrum of the complex substantiates the presence of O–H groups. The sharp band indicative of the N–H vibration of $H_2L{\cdot}H_2O$ is located at 3210 cm^{-1}, and the intense band indicative of the C=O vibration is located at 1652 cm^{-1} in the spectrum of $H_2L{\cdot}H_2O$, which are absent in the complex, indicating the enolisation of the amide group and subsequent proton replacement by the V atom. The strong absorption bands at 1609 cm^{-1} for $H_2L{\cdot}H_2O$ and 1600 cm^{-1} for the complex are assigned to the azomethine ν(C=N).[32] The typical absorption at 972 cm^{-1} of the complex can be assigned to the V=O vibration.[33]

The UV-Vis spectra of $H_2L{\cdot}H_2O$ and the complex were recorded in 10^{-5} mol·L^{-1} in methanol and acetonitrile, respectively, in the range 200–600 nm. The complex shows band centered at 354 nm and weak band at 460 nm. The weak band is attributed to intramolecular charge transfer transitions from the p_π orbital on the nitrogen and oxygen to the empty *d* orbitals of the metal.[34] The intense bands observed at 280 nm for the complex and 298 nm for $H_2L{\cdot}H_2O$ are assigned to intraligand π–π* transitions.[34]

3. 5. Thermal Stability

Thermal analysis was conducted to examine the stability of the complex (Fig. 5). The complex decomposed from 160 °C and completed at 430 °C, with the final product of V_2O_5. The total observed weight loss of 82.3%, corresponding to the total organic part of the complex, is in accordance with the calculated value of 81.6%.

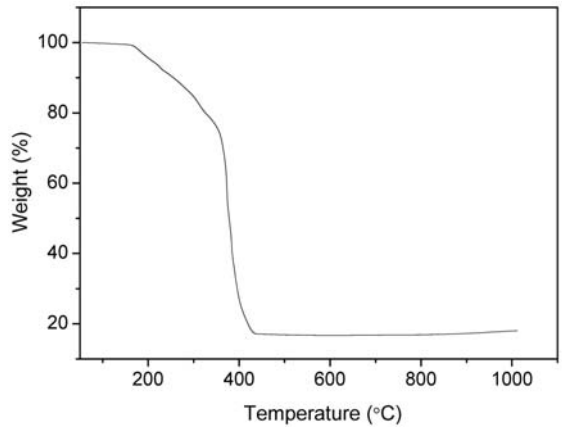

Figure 5. TG-DTA curves of the complex.

3. 6. Glucose Uptake in the Presence of the Complex

Glucose level is a key diagnostic parameter for many metabolic disorders. Biovision glucose assay kit provides direct measurement of glucose in various biological samples. The glucose enzyme mix specifically oxidizes glucose to generate a product, which reacts with a dye to generate color. The generated color is proportional to the glucose amount. The method is rapid, simple, sensitive, and suitable for high throughput.[14] The insulin-like activity of vanadium compounds is usually related to their ability to lower the blood glucose level by activating the glucose transport into the cell of the peripheral tissues. In this study, we have investigated the *in vitro* glucose uptake by C2C12 muscle cells following exposure to the complex. The results are given in Table 5.

Insulin-mimetic test on C2C12 muscle cells indicates that the complex significantly stimulated cell glucose utilization with cytotoxicity at 0.11 g L^{-1}. In general, the insulin enhancing activity of the complex is similar to the reference drugs Insulin and Metformin. So, it is a promising vanadium-based insulin-like material.

Table 5. Glucose uptake in C2C12 cell line results[b]

Compound	Percentage in glucose utilization
DMSO	100
The complex	127 ± 8
Insulin	141 ± 15
Metformin	146 ± 13

[b] The results show the uptake of glucose from the culture media containing 8.0 mmol L^{-1} glucose by C2C12 cells over one 1 h. C2C12 cells were pre-exposed to the compounds, in glucose and serum-free media for 3 h before the glucose uptake experiments. Basal glucose uptake for solvent vehicle only (DMSO) is represented as 100% and the subsequent increase or decrease induced by the compounds is reflected as ±100%.

4. Conclusion

A new hydrazone compound, 4-fluoro-*N*'-(2-hydroxy-3-methoxybenzylidene)benzohydrazide monohydrate, and a new oxidovanadium(V) complex with the hydrazone and kojic acid as ligands were prepared and characterized. The vanadium complex is the first structurally characterized vanadium complex of kojic acid. Insulin-mimetic tests on C2C12 muscle cells indicate that the complex significantly stimulated cell glucose utilization with cytotoxicity at 0.11 g L^{-1}.

5. Supplementary Information

Crystallographic data for the structural analysis has been deposited with the Cambridge Crystallographic Data Centre (CCDC-1477846 for $H_2L \cdot H_2O$ and 1477845 for the complex). Copy of this information can be obtained free of charge from The Director, CCDC, 12 Union Road, Cambridge CB2 1EZ, UK (fax: +44 1223 336 033; e-mail: deposit@ccdc.cam.ac.uk or www: http://www.ccdc.cam.ac.uk).

6. References

1. S. I. Pillai, S. P. Subramanian, M. Kandaswamy, *Eur. J. Med. Chem.* **2013**, *63*, 109–117. http://dx.doi.org/10.1016/j.ejmech.2013.02.002
2. J. J. Smee, J. A. Epps, K. Ooms, S. E. Bolte, T. Polenova, B. Baruah, L. Q. Yang, W. J. Ding, M. Li, G. R. Willsky, *J. Inorg. Biochem.* **2009**, *103*, 575–584. http://dx.doi.org/10.1016/j.jinorgbio.2008.12.015
3. D. Sanna, G. Micera, E. Garribba, *Inorg. Chem.* **2013**, *52*, 11975–11985. http://dx.doi.org/10.1021/ic401716x
4. L. He, X. S. Wang, C. Zhao, D. S. Zhu, W. H. Du, *Metallomics* **2014**, *6*, 1087–1096. http://dx.doi.org/10.1039/c4mt00021h
5. D. C. Crans, A. M. Trujillo, P. S. Pharazyn, M. D. Cohen, *Coord. Chem. Rev.* **2011**, *255*, 2178–2192. http://dx.doi.org/10.1016/j.ccr.2011.01.032
6. A. Sheela, S. M. Roopan, R. Vijayaraghavan, *Eur. J. Med. Chem.* **2008**, *43*, 2206–2210. http://dx.doi.org/10.1016/j.ejmech.2008.01.002
7. Y. Zhang, X. D. Yang, K. Wang, D. C. Crans, *J. Inorg. Biochem.* **2006**, *100*, 80–87. http://dx.doi.org/10.1016/j.jinorgbio.2005.10.006
8. A. Dornyei, S. Marcao, J. C. Pessoa, T. Jakusch, T. Kiss, *Eur. J. Inorg. Chem.* **2006**, *18*, 3614–3621. http://dx.doi.org/10.1002/ejic.200600385
9. M. Haratake, M. Fukunaga, M. Ono, M. Nakayama, *J. Biol. Inorg. Chem.* **2005**, *10*, 250–258. http://dx.doi.org/10.1007/s00775-005-0634-8
10. J. H. McNeill, V. G. Yuen, H. R. Hoveyda, C. Orvig, *J. Med. Chem.* **1992**, *35*, 1489–1491. http://dx.doi.org/10.1021/jm00086a020
11. V. G. Yuen, C. Orvig, J. H. McNeill, *Can. J. Physiol. Pharmacol.* **1993**, *71*, 263–269. http://dx.doi.org/10.1139/y93-041
12. V. G. Yuen, C. Orvig, K. H. Thompson, J. H. McNeill, *Can. J. Physiol. Pharmacol.* **1993**, *71*, 270–276. http://dx.doi.org/10.1139/y93-042
13. S. Fujimoto, K. Fujii, H. Yasui, *J. Clin. Biochem. Nutr.* **1997**, *23*, 113–129. http://dx.doi.org/10.3164/jcbn.23.113
14. A. A. Nejo, G. A. Kolawole, A. R. Opoku, C. Muller, J. Wolowska, *J. Coord. Chem.* **2009**, *62*, 3411–3424. http://dx.doi.org/10.1080/00958970903104327
15. M.-J. Xie, X.-D. Yang, W.-P. Liu, S.-P. Yan, Z.-H. Meng, *J. Inorg. Biochem.* **2010**, *104*, 851–857. http://dx.doi.org/10.1016/j.jinorgbio.2010.03.018
16. M. Amir, I. Ali, M. Z. Hassan, N. Mulakayala, *Archiv. de Pharmazie* **2014**, *347*, 958–968. http://dx.doi.org/10.1002/ardp.201400045
17. G. Rajitha, K. V. S. R. G. Prasad, A. Umamaheswari, D. Pradhan, K. Bharathi, *Med. Chem. Res.* **2014**, *23*, 5204–5214. http://dx.doi.org/10.1007/s00044-014-1091-0
18. M. A. A. El-Sayed, N. I. Abdel-Aziz, A. A. M. Abdel-Aziz, A. S. El-Azab, Y. A. Asiri, K. E. H. ElTahir, *Bioorg. Med. Chem.* **2011**, *19*, 3416–3424. http://dx.doi.org/10.1016/j.bmc.2011.04.027
19. T. Horiuchi, J. Chiba, K. Uoto, T. Soga, *Bioorg. Med. Chem. Lett.* **2009**, *19*, 305–308. http://dx.doi.org/10.1016/j.bmcl.2008.11.090
20. M. Zhang, D.-M. Xian, H.-H. Li, J.-C. Zhang, Z.-L. You, *Aust. J. Chem.* **2012**, *65*, 343–350.
21. Bruker, SMART and SAINT. Bruker AXS Inc., Madison, Wisconsin, USA, **2002**.
22. G. M. Sheldrick, SADABS. Program for Empirical Absorption Correction of Area Detector, University of Göttingen, Germany, **1996**.
23. G. M. Sheldrick, *Acta Crystallogr.* **2008**, *A64*, 112–122. http://dx.doi.org/10.1107/S0108767307043930
24. J. Cui, H. Yin, Y. Qiao, *Acta Crystallogr.* **2007**, *E63*, o3548.
24. R. Dinda, P. Sengupta, S. Ghosh, H. Mayer-Figge, W. S. Sheldrick, *J. Chem. Soc. Dalton Trans.* **2002**, 4434–4439. http://dx.doi.org/10.1039/b207129k
25. J.-Q. Ren, Q.-Z. Jiao, Y.-N. Wang, F.-Y. Xu, X.-S. Cheng, Z.-L. You, *Chinese J. Inorg. Chem.* **2014**, *30*, 640–648.
26. Y. Zhao, X. Han, X.-X. Zhou, H.-H. Li, Z.-L. You, *Chinese J. Inorg. Chem.* **2013**, *29*, 867–874.
27. G.-H. Sheng, X.-F. Chen, J. Li, J. Chen, Y. Xu, Y.-W. Han, T. Yang, Z. You, H.-L. Zhu, *Acta Chim. Slov.* **2015**, *62*, 940–946. http://dx.doi.org/10.17344/acsi.2015.1770
28.vK.-H. Yang, *Acta Chim. Slov.* **2014**, *61*, 629–636.
29. S.-S. Qian, X. Zhao, J. Wang, Z. You, *Acta Chim. Slov.* **2015**, *62*, 828–833.
30. M. He, Q.-Z. Jiao, X.-F. Chen, J. Li, J. Chen, G.-H. Sheng, Z.-L. You, *Chinese J. Inorg. Chem.* **2015**, *31*,1590–1596.
31. Z.-L. You, D.-M. Xian, M. Zhang, *CrystEngComm* **2012**, *14*, 7133–7136. http://dx.doi.org/10.1039/c2ce26201k
32. N. R. Sangeetha, V. Kavita, S. Wocadlo, *J. Coord. Chem.*

2000, *51*, 55–66.
http://dx.doi.org/10.1080/00958970008047078
33. G. Asgedom, A. Sreedhara, J. Kivikoski, E. Kolehmainen, C. P. Rao, *J. Chem. Soc. Dalton Trans.* **1996**, *1*, 93–97.
http://dx.doi.org/10.1039/dt9960000093
34. A. Sarkar, S. Pal, *Polyhedron* **2007**, *26*, 1205–1210.
http://dx.doi.org/10.1016/j.poly.2006.10.012

Povzetek

Sintetizirali smo 4-fluoro-*N*'-(2-hidroksi-3-metoksibenziliden)benzohidrazid monohidrat ($H_2L{\cdot}H_2O$) in ga okarakterizirali z elementno analizo, HRMS, IR, UV-Vis in ^{1}H NMR spektroskopijo. Pri reakciji H_2L, kojične kisline (5-hidroksi-2-(hidroksimetil)-4*H*-piran-4-on; Hka) in $VO(acac)_2$ v metanolu nastane nov oksidovanadijev(V) kompleks, [VO(ka)L]. Kompleks smo okarakterizirali z elementno analizo, IR, UV-Vis in ^{1}H NMR spektroskopijo. Izvedli smo tudi termično analizo. Strukturi H_2L in kompleksa sta bili dodatno potrjeni z monokristalno rentgensko analizo. Vanadijev kompleks je prvi strukturno okarakteriziran vanadijev kompleks s kojično kislino. Inzulinomimetični test na C2C12 mišičnih celicah je pokazal, da kompleks opazno stimulira presnovo glukoze s citotoksičnostjo pri 0.11 g L^{-1}.